$$\frac{\lambda_1}{kC_1Z} = \tan 2\pi L_1/\lambda_1. \quad (9)$$

For a homogeneous resonator constructed from a single material, the capacitance C_1 changes linearly with temperature while Z remains constant.

$$\left[\tan \frac{2\pi L_1}{\lambda_1}\right] \frac{\lambda_2/\lambda_1}{(1+\alpha T)} = Y_{11} \frac{\lambda_2/\lambda_1}{(1+\alpha T)}. \quad (10)$$

The subscripts 1 and 2 designate the initial and final temperatures, respectively. The solution to (10) occurs when

$$\frac{\Delta\lambda}{\lambda_1} = \alpha \Delta T. \quad (11)$$

Consider the case of a composite resonator constructed from two different materials, say a brass outer conductor and a low-expansion inner conductor. After a change in temperature, ΔT, the resonance condition is described by

$$\tan\left[2\pi \frac{L_1}{\lambda_1}\frac{\lambda_1}{\lambda_2}(1+\alpha(a)\Delta T)\right] = Y_{11}\frac{\lambda_2}{\lambda_1}\frac{C_1}{C_2}\frac{Z_1}{Z_2} \quad (12)$$

where C_1 and C_2 are given by (4) and (5), respectively, and Z_1 and Z_2 are given by (6) and (7). This equation cannot be solved as simply as (10), due to the complex temperature dependence of C_2 and the presence of the impedance term on the right-hand side of the equation.

This equation was solved, using Newton's approximation method, on a digital computer for two conditions. These conditions are for a b/a ratio of 3.6 to 1 with $a=0.9$ cm, and a b/a ratio of 9.0 to 1 with $a=0.36$ cm. The results of these solutions are plotted in Figs. 4–7 for a brass outer conductor and various expansion inner conductors for different initial loading factors. It is evident from the curves that the resonator stability deteriorates rapidly for even slight loading of a resonator with a very low-expansion center conductor. For higher-expansion center conductors, the effect is decreased. For an inner-conductor expansion of 2 parts in 10^5 equal to the brass outer conductor, the stability is equal to the material expansion and independent of the loading as it should be.

Example

A composite coaxial resonator was constructed with a low-expansion center conductor and a brass outer conductor. The diameter ratio was 3.6 to 1 and the radius of the inner conductor was 0.9 cm. At room temperature, resonance occurred at 1.385 GHz compared to an unloaded length corresponding to 1.75 GHz. This is a loading factor l_1/λ of 0.198. Between 25°C and 70°C, the inner conductor had a measured expansion of about 5 parts in 10^7. From Fig. 5, this corresponds to a stability $\Delta\lambda/\lambda$ of 2.2 parts in 10^6. The measured stability of the resonator over this range is 3.8 parts in 10^6. This is good correlation with the small discrepancy possibly due to measurement inaccuracy or additional external influences on the resonator.

L. C. Gunderson
Electronic Research Lab.
Corning Glass Works
Raleigh, N. C.

Isolation of Lossy Transmission Line Hybrid Circuits

I. Introduction

With the advent of integrated microwave circuit techniques, use of lossy transmission lines to achieve miniaturization can seriously affect circuit performance. A frequently used performance characteristic of hybrid circuits is the isolation between conjugate ports. Such isolation is normally limited to maximum values of 40 dB to 50 dB due to incidental mismatch of terminations and capabilities of test equipment. When lossy transmission lines are employed to realize the hybrid circuits, an additional constraint is placed upon the peak isolation that can be achieved. In this correspondence, the theoretical isolations of lossy hybrids will be determined at their design center frequencies. Two different hybrid circuits will be considered: the square hybrid and the "rat race" hybrid ring. The preferred method of analysis of symmetrical four-port networks will be used herein.[1]

To analyze the lossy hybrids, one must use the complex propagation constant γ, where $\gamma=\alpha+j\beta$. The attenuation per unit length is nepers per unit length is α, while β is the phase shift per unit length in radians per unit length. Three trigonometric identities will be used:[2,3]

$$\tanh\left(\frac{\gamma L}{2}\right) = \frac{\cosh(\gamma L)-1}{\sinh(\gamma L)} \quad (1)$$

$$\sinh(\gamma L) = \sinh(\alpha L + j\beta L) = \sinh \alpha L \cos \beta L + j \cosh \alpha L \sin \beta L \quad (2)$$

$$\cosh(\gamma L) = \cosh(\alpha L + j\beta L) = \cosh \alpha L \cos \beta L + j \sinh \alpha L \sin \beta L. \quad (3)$$

For a quarter-wave transmission line of small dissipation, $L=\lambda/4$, $\sinh \alpha L \cong \alpha L$, $\cosh \alpha L \cong 1$, $\sin \beta L \cong 1$, and $\cos \beta L \cong 0$:

Then

$$\left.\begin{aligned} \sinh(\gamma L) &\cong j \\ \cosh(\gamma L) &\cong j\,\alpha L \\ \tanh\left(\frac{\gamma L}{2}\right) &\cong \alpha L + j \end{aligned}\right\}. \quad (4)$$

For a three-quarter-wave transmission line of small dissipation, $3L=3\lambda/4$, $\sinh 3\alpha L \cong 3\alpha L$, $\cosh 3\alpha L \cong 1$, $\sin 3\beta L \cong -1$, and $\cos 3\beta L \cong 0$. Then

$$\left.\begin{aligned} \sinh(3\gamma L) &\cong -j \\ \cosh(3\gamma L) &\cong -j3\alpha L \\ \tanh\left(\frac{3\gamma L}{2}\right) &\cong 3\alpha L - j \end{aligned}\right\}. \quad (5)$$

II. Square Hybrid

The square hybrid (see Fig. 1) uses four quarter-wave transmission lines. The *ABCD* matrix for this hybrid can be found for both the even $(M{+}{+})$ and the odd $(M{+}{-})$ modes:

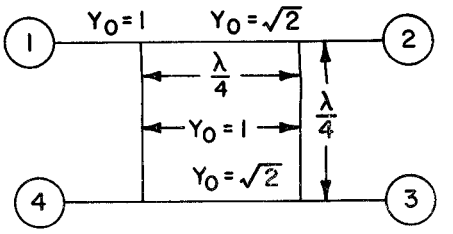

Fig. 1. Square hybrid.

$$M_{+\pm} = \begin{bmatrix} 1 & 0 \\ Y_{+\pm} & 1 \end{bmatrix} \times \begin{bmatrix} \cosh(\gamma_2 L) & \frac{1}{\sqrt{2}}\sinh(\gamma_2 L) \\ \sqrt{2}\sinh(\gamma_2 L) & \cosh(\gamma_2 L) \end{bmatrix} \times \begin{bmatrix} 1 & 0 \\ Y_{+\pm} & 1 \end{bmatrix} \quad (6)$$

where

γ_2 = propagation constant per unit length of transmission lines connecting ports 1 and 2, and ports 4 and 3,

$y_{+\pm}$ are admittances of shunt stubs for even and odd modes.

For the even mode: (shunt stubs are open-circuited)

$$Y_{++} = Y_0 \tanh\left(\frac{\gamma_1 L}{2}\right) \quad (7)$$

where

γ_1 = propagation constant per unit length of transmission lines connecting ports 1 and 4, and ports 2 and 3.

Letting $Y_0=1$, and substituting (4) into (7)

$$Y_{++} = \alpha_1 L + j. \quad (8)$$

For the odd mode: (shunt stubs are short-circuited)

$$Y_{+-} = \frac{Y_0}{\tanh\left(\frac{\gamma_1 L}{2}\right)}. \quad (9)$$

Letting $Y_0=1$ and substituting (4) into (9)

$$Y_{+-} = \frac{1}{\alpha_1 L + j} = \frac{\alpha_1 L - j}{(\alpha_1 L)^2 + 1}. \quad (10)$$

For small dissipation, $(\alpha_1 L)^2 \ll 1$ then

$$Y_{+-} \cong \alpha_1 L - j. \quad (11)$$

Substituting (4), (8), and (11) into (6), it can be shown that

$$M_{+\pm} = j\begin{bmatrix} 1 & 0 \\ \alpha_1 L \pm j & 1 \end{bmatrix} \times \begin{bmatrix} \alpha_2 L & \frac{1}{\sqrt{2}} \\ \sqrt{2} & \alpha_2 L \end{bmatrix} \times \begin{bmatrix} 1 & 0 \\ \alpha_1 L \pm j & 1 \end{bmatrix}. \quad (12)$$

Performing the matrix multiplications in (12) and disregarding all second-order terms involving $\alpha_1 L$ and $\alpha_2 L$:

Manuscript received June 21, 1966; revised September 12, 1966.

[1] J. Reed and G. J. Wheeler, "A method of analysis of symmetrical four-port networks," *IRE Trans. on Microwave Theory and Techniques*, vol. MTT-4, pp. 246–252, October 1956.

[2] J. D. Ryder, *Networks, Lines, & Fields*. Englewood Cliffs, N. J : Prentice-Hall, 1949, p. 200.

[3] *Reference Data for Radio Engineers*, 4th Ed. New York: IT&T Corp., 1956, p. 1949.

$$M_{+\pm} = \begin{bmatrix} A & B \\ C & D \end{bmatrix} = j \begin{bmatrix} \frac{\alpha_1 L}{\sqrt{2}} + \alpha_2 L \pm j\frac{1}{\sqrt{2}} & \frac{1}{\sqrt{2}} \\ \pm\frac{2j\alpha_1 L}{\sqrt{2}} \pm 2j\frac{\alpha_2 L}{\sqrt{2}} + \sqrt{2} - \frac{1}{\sqrt{2}} & \frac{\alpha_1 L}{\sqrt{2}} + \alpha_2 L \pm j\frac{1}{\sqrt{2}} \end{bmatrix} \quad (13)$$

now,

$$\Gamma = \frac{A + B - C - D}{A + B + C + D} = \text{voltage reflection coefficient} \quad (14)$$

$$\Gamma_{+\pm} = \frac{\frac{2}{\sqrt{2}} - \sqrt{2} \mp \frac{2j\alpha_1 L}{\sqrt{2}} \mp 2j\alpha_2 L}{\sqrt{2} \pm j\frac{2}{\sqrt{2}} + \frac{2\alpha_1 L}{\sqrt{2}} + 2\alpha_2 L \pm \frac{2j\alpha_1 L}{\sqrt{2}} \pm 2j\alpha_2 L}. \quad (15)$$

Letting A_4 equal the vector amplitude of the signal emerging from port 4,

$$A_4 = \tfrac{1}{2}[\Gamma_{++} - \Gamma_{+-}]. \quad (16)$$

Substituting (16) into (15) and discarding all second-order terms involving $\alpha_1 L$ and $\alpha_2 L$, it can be shown that

$$A_4 = -j\left[\frac{\alpha_1 L + \sqrt{2}\,\alpha_2 L}{2 + 4\alpha_1 L + 4\sqrt{2}\,\alpha_2 L}\right]. \quad (17)$$

Now

$$I = 20 \log_{10}\left|\frac{1}{A_4}\right| \quad (18)$$

where I=isolation is dB

$$I = 20\log_{10}\left[\frac{2 + 4\alpha_1 L + 4\sqrt{2}\,\alpha_2 L}{\alpha_1 L + \sqrt{2}\,\alpha_2 L}\right]$$

$$\cong 20\log_{10}\left[\frac{2}{\alpha_1 L + \sqrt{2}\,\alpha_2 L}\right]. \quad (19)$$

III. "Rat Race" Hybrid Ring

The "rat race" hybrid ring (see Fig. 2) uses three quarter-wave (i.e., $\lambda/4$) transmission lines and one three-quarter-wave (i.e., $\frac{3}{4}\lambda$) transmission line. The same method of analysis previously used for the lossy square hybrid is directly applicable.

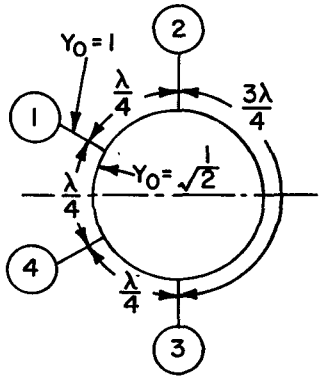

Fig. 2 "Rat race" hybrid ring.

Since the first shunt stub of the bisected network is an eighth-wavelength long, (7), (8), (9), (10), and (11) are applicable when $Y_0 = 1/\sqrt{2}$ and $\alpha_1 = \alpha$. Then

$$Y_{1+\pm} = \frac{\alpha L}{\sqrt{2}} \pm j\frac{1}{\sqrt{2}}; \quad (20)$$

for the second shunt stub

$$Y_{2++} = Y_0 \tanh\left(\frac{3\gamma L}{2}\right). \quad (21)$$

Letting $Y_0 = 1/\sqrt{2}$ and substituting (5) into (21),

$$Y_{2++} = 3\alpha L - j \quad (22)$$

now

$$Y_{2+-} = \frac{Y_0}{\tanh\left(\frac{3\gamma L}{2}\right)}. \quad (23)$$

Letting $Y_0 = 1/\sqrt{2}$ and substituting (5) into (23)

$$Y_{2+-} = \frac{1}{\sqrt{2}}\left(\frac{1}{3\alpha L - j}\right) = \frac{1}{\sqrt{2}}\left(\frac{3\alpha L + j}{(3\alpha L)^2 + 1}\right). \quad (24)$$

For small dissipation,

$$(3\alpha L)^2 \ll 1;$$

then

$$Y_{2+-} \cong \frac{3\alpha L}{\sqrt{2}} + \frac{j}{\sqrt{2}}. \quad (25)$$

The $ABCD$ matrix for the "rat race" hybrid ring can be evaluated using (20), (22), and (25) for $Y_{1+\pm}$ and $Y_{2+\pm}$. Upon determining the vector amplitude of the signal emerging from port 3 and discarding all second-order terms involving αL, it can be shown that

$$I = 20\log_{10}\left[\frac{4 + 12\sqrt{2}\,\alpha L}{\sqrt{2}\,\alpha L}\right]$$

$$\cong 20\log_{10}\left[\frac{2.83}{\alpha L}\right]. \quad (26)$$

IV. Numerical Results

The unloaded Q of a resonant length of lossy transmission line can be related conveniently to the attenuation per unit length when the dissipation is small:[4]

$$Q = \frac{\beta}{2\alpha} = \frac{\pi}{\lambda\alpha}, \quad (27)$$

where λ=wavelength. Rearranging terms and letting $L = \lambda/4$, it can be shown that

$$\alpha L = \frac{\pi}{4Q} = \frac{0.785}{Q}. \quad (28)$$

[4] E. C. Jordan, *Electromagnetic Waves and Radiating Systems*. Englewood Cliffs, N. J.: Prentice-Hall, 1950, pp. 236–239.

Using (19), (26), and (28), theoretical hybrid isolations have been calculated for Q's of 10, 100, 1000, and ∞. These numerical results are tabulated below:

Q	L	I (Square Hybrid)	I ("Rat Race" Hybrid Ring)
10	0.0785	23.3 dB	33.7 dB
100	0.00785	40.8 dB	51.4 dB
1000	0.000785	60.5 dB	71.1 dB
∞	0	dB	dB

(Note: $\alpha_1 = \alpha_2 = \alpha$ is assumed for the square hybrid.)

For the square hybrid when $\alpha_1 = \alpha_2 = \alpha$

$$I = 20\log_{10}\left[\frac{2 + 9.66\alpha L}{2.414\alpha L}\right]$$

$$\cong 20\log_{10}\left[\frac{0.83}{\alpha L}\right]. \quad (29)$$

Upon comparing (26) and (29), it can be seen that as αL approaches zero, the isolation of the "rat race" hybrid ring will be 10.6 dB greater than the isolation of the square hybrid for the same αL in both hybrids. Such a performance advantage is not unexpected since the bandwidth of the square hybrid is less than that of the "rat race" hybrid ring.[1] Isolation in hybrid circuits is similar to peak rejection in a band-reject filter. As filter bandwidths become wider, the same amount of incidental dissipation (i.e., same resonator unloaded Q) results in higher peak rejection.

R. M. Kurzrok
Advanced Communications Lab.
RCA
New York, N. Y.

A Stepped Mode Transducer Using Homogeneous Waveguides

***Abstract*—A rectangular to cylindrical waveguide transducer is described which couples the dominant rectangular (TE_{10}) and dominant cylindrical (TE_{11}°) modes. The maximum voltage reflection coefficient remains less than 0.025 over the design bandwidth. Symmetry considerations substantiated by moding tests show the transducer to be higher-order mode free. Previous work is reviewed, the design method discussed, and experimental data shown.**

Broadband rectangular to dominant mode cylindrical waveguide transducers are common to several devices in the microwave region, most notable of which is perhaps the precision rotary vane attenuator. Frequently such transducers are realized by construction of a taper section several wavelengths in size. As a result of a recent study of the dominant

Manuscript received June 28, 1966. This paper presents the results of one phase of research carried out at the Jet Propulsion Lab., California Institute of Technology, Pasadena, Calif., under Contract NAS7-100, sponsored by the National Aeronautics and Space Administration.